

Hypernuclear physics with electron beams: Exclusive and inclusive excitations

Joseph Cohen

Department of Physics, University of Virginia, Charlottesville, Virginia 22901

(Received 11 March 1985)

We discuss the importance of the $A(e, e'K^+)_{\Lambda}A^*$ in hypernuclear physics, comparing it with the $A(K^-, \pi^-)_{\Lambda}A^*$ reaction and suggesting problems that can preferentially be studied with the $(e, e'K^+)$ probe. Cross sections are given for exclusive and inclusive processes for a large range of nuclear masses. The elementary process $p(e, e'K^+)\Lambda$ is not well known, and the coupling constants and electromagnetic moments are discussed.

I. INTRODUCTION

Hypernuclear physics is currently an important and interesting area of nuclear science.¹⁻¹³ An interesting bound nuclear system with strangeness $S = -1$ is the Λ hypernucleus ($_{\Lambda}A$), in which a Λ -hyperon replaces one of the nucleons. This system is long lived ($\sim 10^{-10}$ sec) and provides a variety of interesting nuclear phenomena.¹⁻¹³

Most of the information on hypernuclei comes from the $A(K^-, \pi^-)_{\Lambda}A$ reaction, studied at CERN, BNL, and KEK. Nevertheless, this reaction has a number of disadvantages: (i) It excites strongly only the natural parity hypernuclear states;¹⁴ (ii) both the K^- and the π^- are strongly absorbed in the nucleus, so that many uncertainties occur when the reaction mechanism and the absorption are considered; (iii) low-spin (natural parity) states dominate the spectrum at forward angles, and the reaction thus emphasizes the spectroscopy of such states. A number of alternative reactions have been proposed,¹⁵⁻¹⁷ and two of them have been studied in detail so far: the (π^+, K^+) (Ref. 16) and the (γ, K^+) (Ref. 18).

In this work we focus our attention on the $(e, e'K^+)$ reaction. Although suggested on several occasions in the past,^{15,17-20} this reaction has not yet been deeply looked into. In this paper we shall first discuss the importance of this reaction, bearing in mind the attributes of the new generation of continuous wave (with high current, and high duty factor) electron accelerators Continuous Electron Beam Accelerator Facility (CEBAF). We then study the $(e, e'K^+)$ reaction [thereby examining the former (γ, K^+) calculations] for both exclusive and inclusive excitations for a series of nuclei from ${}^4\text{He}$ to ${}^{208}\text{Pb}$. We shall indicate that the elementary $p(e, e'K^+)\Lambda$ process is itself not well known, and also discuss the $K^+\Lambda p$ vertex function (form factor). In studying the nuclear reaction we shall employ a transition amplitude that goes beyond the lowest-order $(\sigma \cdot \hat{\epsilon})$ term used in previous calculations, and treat also non-spin-flip excitations. A preliminary presentation of part of the present treatment is given in Ref. 21.

II. WHY $(e, e'K^+)$?

The $A(e, e'K^+)_{\Lambda}A$ reaction excites both natural and unnatural parity hypernuclear states with comparable

strength. Since the electrons, and especially the K^+ meson, are very weakly absorbed in the nucleus, the theoretical analysis of the reaction is relatively reliable compared with reactions involving the K^- meson and pions. The weak absorption does not confine the $(e, e'K^+)$ reaction to the nuclear surface and provides the possibility of studying hypernuclear states with a deeply-bound Λ hyperon. Unlike typical K^- beams, with ten times more unwanted particles than kaons, electron beams are very "clean" and well under control. In heavy nuclei the reaction would provide the necessary tool to probe the behavior of the Λ in nuclear matter. It may also be used in such heavy nuclei as a means to study the possible modification of the electromagnetic currents [which might be suggested by quasi- and deep-inelastic electron scattering²² and by the European Muon Collaboration (EMC) data²³]. The reaction would be extremely useful in measuring the magnetic moment of a deeply-bound hyperon using the reaction ${}^{209}\text{Bi}(e, e'K^+)_{\Lambda}{}^{209}\text{Pb}$ (in order to compare it with that of a free Λ), because (i) the electron beam will have a high intensity and will be relatively very narrow, therefore the measurement is expected to be practical (unlike the case with the very wide K^- beam); (ii) one can produce a polarized electron beam, whereas no polarized K^- 's can be used; (iii) the high momentum transfer in the reaction, which is unavoidable under the kinematical circumstances, helps in this case to enhance the required direct transition from the valence proton in ${}^{209}\text{Bi}$ to a $1s$ Λ particle in the ${}^{209}_{\Lambda}\text{Pb}$ hypernucleus (the overlap of the wave functions is larger here). In addition, the $(e, e'K^+)$ reaction on typical nuclei excites only high isospin states ($T_f = T_i + \frac{1}{2}$). We also believe that the contrast of $(e, e'K^+)$ with $(e, e'\pi^{\pm})$ ($m_K \gg m_{\pi}$, and no soft-meson theory is expected to be applicable) should be revealing, and plan to study these topics successively.

The transition operator involved has a spin part, and the reaction is thus a possible probe of spin-flip, $\Delta T = \frac{1}{2}$ states (for example, $J^P = 0^+ \rightarrow J^P = 1^+$, $T = \frac{1}{2}$ in ${}^{12}\text{C}$, or $0^+ \rightarrow 0^-$ in ${}^{90}\text{Zr}$). It is well known that spin-isospin excitations present a number of theoretical puzzles such as a universal, hitherto unexplained quenching of the transition strength at low momentum transfers (observed in numerous transitions with a variety of probes), or, at

higher momentum transfer, expected contrast, when the spin-longitudinal and spin-transverse responses are compared. Similar quenching phenomena have surprisingly been observed lately for isoscalar transitions ($\Delta T=0$) as well,^{24,25} and it would be extremely interesting to look for such effects also for $\Delta T=\frac{1}{2}$, in addition to $\Delta T=0,1$. It is suggested that the $(e,e'K^+)$ reaction can be used as a probe for this study at high momentum transfers (the low-momentum-transfer data being obtained from complementary hypernuclear reactions).

In addition to the above features, the $(e,e'K^+)$ reaction has another (well known) advantage over the (γ,K^+) one. As is well known, the information extracted from photon reactions is limited, because the photon energy and momentum are equal. This shortcoming is avoided if the reaction is induced by electrons.

III. THE ELEMENTARY TRANSITION OPERATOR

A. Feynman diagrams for $e + p \rightarrow e' + K^+ + \Lambda$

The nuclear $A(e,e'K^+)_{\Lambda}A^*$ reaction is presented diagrammatically in Fig. 1(a) where the kinematics is defined. The blob in the right vertex of Fig. 1(a) is treated based on the three Feynman diagrams of Figs. 1(b)–(d). They consist of Born terms in the s , t , and u channels with the exchange of a proton, a kaon, and the two hyperons Λ and Σ^0 , respectively. We have not included the contribution of higher strange meson resonances (such as the K^*) or hyperon resonances (such as the Y^*). These are not expected to be important for medium-energy kaons production. In fact, for threshold K^+ production the reaction is dominated by the catastrophic term,²⁶ that is, by a three-dimensional current \mathbf{J} resulting from the proton-pole Born term of Fig. 1(c). Hsiao and Cotanch¹⁸ find the K^* contribution to be less than that of the Σ^0

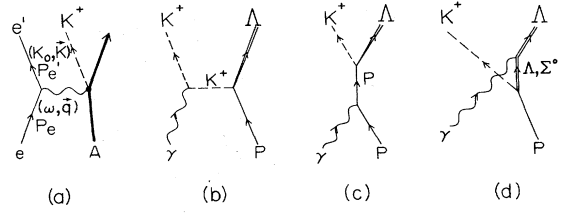


FIG. 1. (a) The nuclear $A(e,e'K^+)_{\Lambda}A^*$ reaction with the kinematical variables for the electrons, photon, and outgoing kaon. (b)–(d) Feynman diagrams for the elementary reaction (only the virtual photon is shown, and electron lines are omitted).

pole, which turns out to be unimportant in our calculations. We note that our theory is equivalent to π electroproduction in pseudoscalar coupling.

B. The baryon current

The various vertex operators associated with the diagrams of Fig. 1 are given by Thom.²⁷ We calculated the electromagnetic current J_{μ} for the elementary process using standard relativistic quantum perturbation theory techniques,²⁸ and then obtained the nonrelativistic reduced form, keeping also important terms of order p/M . Our present amplitude goes beyond previous calculations^{17–19} that use only the lowest-order ($\sigma \cdot \hat{\mathbf{e}}$) term. (Nevertheless, we note that a fully relativistic formalism should probably be used for high momentum transfers. Such a program is currently under consideration.)

The nonrelativistic form used for the current J^{μ} is

$$J^0 = -\frac{g_{K\Lambda p} e}{(M_{\Lambda} - M_N)^2 - m_{K^+}^2} (2K_0 - \omega) \frac{\sigma \cdot (\mathbf{K} - \mathbf{q})}{M_N + M_{\Lambda}} - \frac{g_{K\Lambda p} e}{q^2 + 2M_N \omega} \sigma \cdot \mathbf{K} + \frac{g_{K\Lambda p} \mu_p}{m_{K^+}^2 + 2M_N K_0} (K_0 + M_{\Lambda} - M_N) \sigma \cdot \mathbf{q} \\ - \frac{g_{K\Lambda p} \mu_{\Lambda}}{M_N^2 - M_{\Lambda}^2 + m_{K^+}^2 - 2M_N K_0} (K_0 + M_{\Lambda} - M_N) \sigma \cdot \mathbf{q} - \frac{g_{K\Sigma^0 p} \mu_T}{M_N^2 - M_{\Sigma^0}^2 + m_{K^+}^2 - 2M_N K_0} (K_0 + M_{\Sigma^0} - M_N) \sigma \cdot \mathbf{q} \quad (1)$$

for $\mu=0$, and

$$\mathbf{J} = -\frac{g_{K\Lambda p} e}{(M_{\Lambda} - M_N)^2 - m_{K^+}^2} (2\mathbf{K} - \mathbf{q}) \frac{\sigma \cdot (\mathbf{K} - \mathbf{q})}{M_N + M_{\Lambda}} + \frac{g_{K\Lambda p} e}{q^2 + 2M_N \omega} \left[i \frac{\mathbf{q} \times \mathbf{K}}{M_N + M_{\Lambda}} - \omega \sigma \right] + \frac{g_{K\Lambda p} \mu_p}{m_{K^+}^2 + 2M_N K_0} \\ \times \{ [(K_0 + M_{\Lambda} - M_N) \omega - \mathbf{K} \cdot \mathbf{q}] \sigma + (\sigma \cdot \mathbf{q}) \mathbf{K} \} - \frac{g_{K\Lambda p} \mu_{\Lambda}}{M_N^2 - M_{\Lambda}^2 + m_{K^+}^2 - 2M_N K_0} \{ [(K_0 + M_{\Lambda} - M_N) \omega - \mathbf{K} \cdot \mathbf{q}] \sigma + (\sigma \cdot \mathbf{q}) \mathbf{K} \} \\ - \frac{g_{K\Sigma^0 p} \mu_T}{M_N^2 - M_{\Sigma^0}^2 + m_{K^+}^2 - 2M_N K_0} \{ [(K_0 + M_{\Sigma^0} - M_N) \omega - \mathbf{K} \cdot \mathbf{q}] \sigma + (\sigma \cdot \mathbf{q}) \mathbf{K} \} \quad (2)$$

for $\mu=1, 2$, or 3 . In Eqs. (1) and (2) the coupling constants of the K meson to the Λp and the $\Sigma^0 p$ vertices are denoted by $g_{K\Lambda p}$ and $g_{K\Sigma^0 p}$, respectively. The proton charge is $e \simeq \sqrt{4\pi/137}$, while the masses are denoted by M_N , $M_{\Lambda} = 1115.6$ MeV, $M_{\Sigma^0} = 1192.5$ MeV, and

$m_{K^+} = 493.7$ MeV for the proton, the Λ and Σ^0 hyperons, and the K^+ strange meson, respectively. Appearing in Eqs. (1) and (2) are the anomalous magnetic moments $\mu_p = 1.79(e/2M_N)$, $\mu_{\Lambda} = -0.613(e/2M_N)$, and the transition moment $\mu_T = \kappa_T e/2M_N$, where κ_T will be discussed

in the following. The current J^μ is exactly gauge invariant in its relativistic covariant form; gauge invariance is maintained up to order p/M in the nonrelativistic reduction.

C. The coupling constants and magnetic moments

There is a considerable uncertainty regarding the values of the coupling constants and the transition moment ($g_{K\Lambda p}$ and $g_{K\Sigma^0 p}$, and μ_T , respectively) of Eqs. (1) and (2). While the magnetic moments are known to a very good degree of accuracy, the rest of the required physical constants are not.

The early work of Thom²⁷ and Kuo²⁹ yielded values which differ substantially from current compilations.³⁰ Theoretical efforts based on a quark model³¹ or a potential approach³² give results in rough agreement only with each other. The transition moment μ_T is currently determined³³ as $\mu_T = -1.82 \pm 0.22$, where the negative sign is extracted from the naive quark model.³⁴

A number of representative sets of values for the physical constants used in this work are presented in Table I; the large variation in the values of these constants is clearly demonstrated. We note, in particular, the large difference between the values of Thom²⁷ and the rest of Table I. The results of Thom²⁷ have recently been employed in a calculation by Hsiao and Cotanch.¹⁸ We shall be interested in pointing out any substantial differences in the predictions of the various sets of constants of Table I, with the hope that comparisons with future experimental measurements can judge which of these should be used.

IV. THE NUCLEAR REACTION

A. The interaction Hamiltonian

The scattering matrix for the nuclear ($e, e'K^+$) reaction can be expressed by means of the interaction Hamiltonian H'_{fi} as

$$S_{fi} = 2\pi i H'_{fi} \delta(E_f - E_i), \quad (3)$$

where the subscripts i and f denote the initial and final states, while E is the total energy. The interaction H'_{fi} is given in terms of the baryon current J^μ , the electromagnetic current j_{em}^μ , and the kinematical variables of Fig. 1(a) as

$$H'_{fi} = \left[\frac{m_e^2}{2\omega_K(m_e^2 + \mathbf{p}_e^2)^{1/2}(m_e^2 + \mathbf{p}_e'^2)^{1/2}} \right]^{1/2} j_{em}^\mu J_\mu, \quad (4)$$

where

$$j_{em}^\mu = -\frac{ie}{\omega^2 - \mathbf{q}^2} \bar{u}_{\sigma'}(p_e') \gamma^\mu u_\sigma(p_e) e^{i(\mathbf{q}-\mathbf{K})\cdot\mathbf{r}}, \quad (5)$$

with $u_{\sigma'}(p_e')$ and $u_\sigma(p_e)$ representing the outgoing and incoming electron Dirac spinors,

$$\omega_K = K_0 = (m_{K^+}^2 + \mathbf{K}^2)^{1/2},$$

and m_e is the electron mass (in what follows, we deal with extremely relativistic electrons; $p_e, p_e' \gg m_e$, and m_e will be neglected).

B. The reaction cross section

The differential cross section for polarized electrons (with polarizations σ' and σ) is

$$\left[\frac{d^3\sigma}{d\Omega_{\hat{\mathbf{p}}_e'} d\Omega_{\hat{\mathbf{K}}} d\omega_K} \right]_{\text{pol}} = \frac{1}{2(2\pi)^5} \frac{p_e' K}{p_e} \left[\frac{em_e}{\omega^2 - \mathbf{q}^2} \right]^2 \times |\bar{u}_{\sigma'}(p_e') \gamma_\mu u_\sigma(p_e) M_{fi}^\mu|^2, \quad (6)$$

where

$$M_{fi}^\mu = \langle f | \sum_{n=1}^Z [J^\mu e^{i(\mathbf{q}-\mathbf{K})\cdot\mathbf{r}}]_n | i \rangle, \quad (7)$$

$d\Omega_{\hat{\mathbf{a}}}$ is a solid angle element around the direction of \mathbf{a} , and the sum goes over all target protons. We have assumed plane waves for the kaon and electrons, since these are very weakly distorted in the nucleus.

The unpolarized cross section is given by summing over σ' and averaging over σ . Using trace and projection techniques²⁸ in summing over σ, σ' , we find,

$$\frac{d^3\sigma}{d\Omega_{\hat{\mathbf{p}}_e'} d\Omega_{\hat{\mathbf{K}}} d\omega_K} = \frac{1}{4(2\pi)^5} \frac{p_e' K}{p_e} \frac{e^2}{(\omega^2 - \mathbf{q}^2)^2} \Gamma_x, \quad (8)$$

where

$$\Gamma_x = 2 \text{Re}[(p_e' \cdot M_{fi})(p_e \cdot M_{fi}^\dagger)] - (p_e' \cdot p_e)(M_{fi} \cdot M_{fi}^\dagger), \quad (9)$$

and the four-dimensional vector products mean, e.g.,

$$p_e' \cdot M_{fi} \equiv p_e' \cdot M_{fi}^\mu \equiv p_e'^0 M_{fi}^0 - \mathbf{p}_e' \cdot \mathbf{M}_{fi}.$$

TABLE I. Representative values for the coupling constants and moments used in this work. The values of μ_p and μ_Λ are well determined and consistently taken to be 1.29 and -0.613 nm, respectively.

Set	$g_{K\Lambda p}/\sqrt{4\pi}$	$g_{K\Sigma^0 p}/\sqrt{4\pi}$	μ_T (nm)
I	+2.50 (Ref. 27)	+2.50 (Ref. 27)	+0.6 (Ref. 27)
II	-4.13 (Ref. 31)	+0.82 (Ref. 31)	-1.82 (Refs. 33, 34)
III	-4.07 (Ref. 32)	+0.26 (Ref. 32)	-1.82
IV	-4.56 (Ref. 30)	+1.00 (Ref. 30)	-1.82
V	-3.73 (Ref. 30)	+0.95 (Ref. 30)	-1.82

We have used the extreme relativistic limit for the electrons, since they have very high energies (up to 4 GeV).

C. The KAN vertex form factor

As is well known, the finite size of the hadrons and off-shell extrapolation of a meson-baryon vertex operator require a vertex form factor. In the pion case one usually adopts either a monopole or a dipole form for such a function. In the present work, we shall test a number of such form factor vertex functions:

(i) The dipole function suggested by Bozoian, van Doremalen, and Weber³¹

$$\Gamma_v(Q^2) = [1 - (Q_0^2 - Q^2)/\Lambda^2]^{-2}, \quad \Lambda \simeq 900 \text{ MeV}, \quad (10)$$

which is supposed to be valid for momentum transfers up to $|Q| \simeq 0.5 \text{ GeV}/c$ (Ref. 31), and is very similar to a Gaussian vertex function³⁵ based on the constituent quark model.³⁶

(ii) The phenomenological off-shell monopole form

$$\Gamma_v(Q^2) = \frac{\Lambda^2 - m_{K^+}^2}{\Lambda^2 - Q_0^2 + Q^2}, \quad (11)$$

where we try both a soft vertex cutoff ($\Lambda = 900 \text{ MeV}$) and a harder one ($\Lambda = 1200 \text{ MeV}$). While the former Λ is somewhat harder than that of Eq. (10), it is still soft enough to be characteristic of quark models. The latter cutoff is a commonly used value for the pion vertex in phenomenological fits, but it is not as large as the cutoff used for the ρ meson ($\Lambda_\rho \simeq 2-2.5 \text{ GeV}$). Possible form factors for the electric charges and the magnetic moments³⁰ can be absorbed in the form factors we have already introduced [Eqs. (10) and (11)].

As far as we know, previous similar works do not include any vertex functions for the KNA interaction. We shall also calculate for such a case, where a local ($\Lambda \rightarrow \infty$) KNA interaction is assumed. In the following sections, we shall compare results based on the different vertex functions discussed.

We note that there is a problem of gauge invariance violation when the form factor vertex functions are introduced, because they are different for each diagram.³⁷ The hyperon-pole diagram [Fig. 1(d)] is gauge invariant by itself and is not a source of problems, but its contribution is unimportant in this particular calculation. The other two diagrams [Figs. 1(b) and (c)] have different form factors for both the $K\Lambda p$ and the γNN vertices. In order to estimate the form factor effects, we invoke a proton-at-rest approximation, and factorize out a common vertex func-

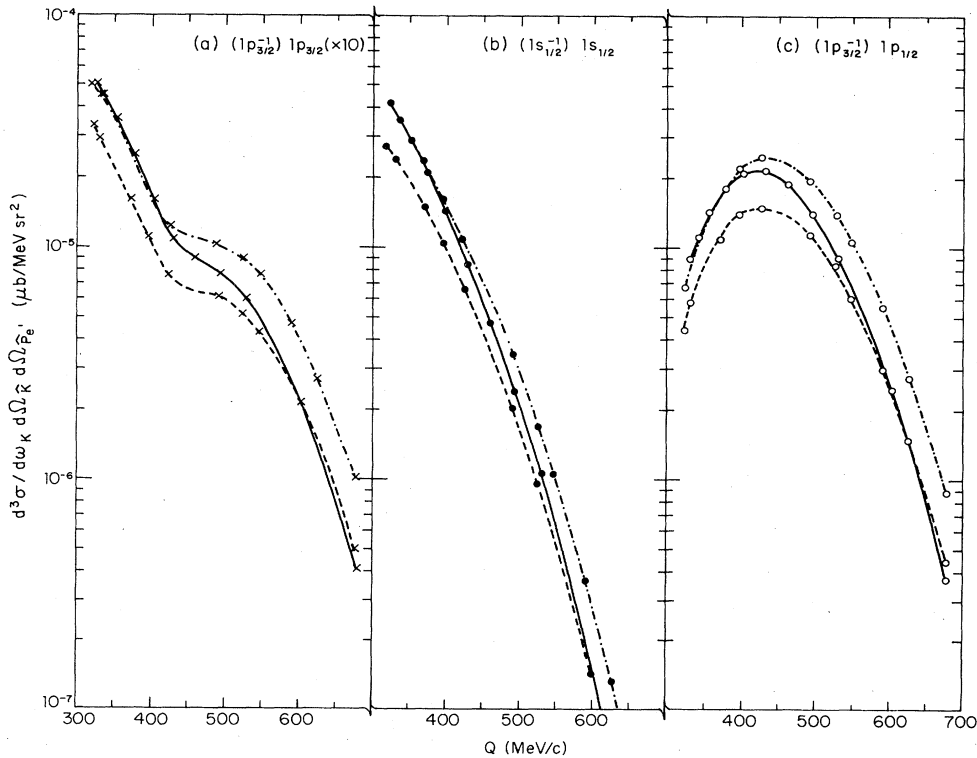


FIG. 2. Exclusive differential cross sections for $^{12}\text{C}(e, e'K^+)^{12}\text{B}^*$ ($J^P=1^+$) for (a) a substitutional state, (b) a deeply-bound Λ hyperon, and (c) a $1A-1h$ configuration which is the dominant one in the case of a nonstrange 1^+ excitation ($1N-1h$ regular shell-model). The three different curves in each case correspond to different form factor vertex functions: The solid curve represents a calculation with the form of Bozoian *et al.* (Ref. 31) [Eq. (10)], the dashed curve is based on using Eq. (11) with $\Lambda = 900 \text{ MeV}$, and the dashed-dotted curve is based on a similar vertex function with $\Lambda = 1200 \text{ MeV}$. The results shown here were calculated using set II of constants in Table I.

tion form factor, maintaining gauge invariance. As we shall see, this contributes an overall reduction factor in the pertinent momentum region. As long as the behavior of the true vertex functions is not dramatically different in the two cases of Figs. 1(b) and (c), we do not expect the contribution of the form factors to be very different from this simple-minded calculation. This problem has not yet been solved in the literature,³⁷ and we believe its implications on the present work are quite limited.

V. EXCITATION OF DISCRETE HYPERNUCLEAR LEVELS

A. General considerations

We calculate the four-vector amplitude M_{fi}^μ of Eq. (7) using the shell model. Each hypernuclear level is characterized by a one-particle-one-hole (1p-1h) shell model configuration.³⁸ We have exploited the harmonic-oscillator wave functions $R_{nl}(r)$ as a handy means for estimating cross sections, despite the high momentum transfers involved. We note that Refs. 16 and 18 find the harmonic-oscillator results to be in surprisingly good agreement with Woods-Saxon cross sections. Since we only intend to have cross section estimates at this point (it

is still five to ten years until a new cw accelerator is operative), this question of Woods-Saxon against harmonic-oscillator wave functions is only of minor importance.

The final three-body state of the nuclear reaction requires a full three-dimensional relativistic kinematical analysis. While a strong dependence of the cross section on the azimuthal angle of the outgoing meson ($\phi_{\hat{K}}$) is not expected at threshold,²⁶ it will be important for higher momenta of the outgoing kaon.

The differential cross section for the reaction $A(e, e'K^+)_{\Lambda}A^*$ is calculated from Eqs. (8) and (9), evaluating M_{fi}^μ from Eq. (7). We calculate for closed-shell nuclei in the mass range from ${}^4\text{He}$ to ${}^{208}\text{Pb}$, where the initial state has the quantum numbers $J^P=0^+$ and $T=T_i$. We characterize the final state by a one-lambda-hyperon-one-nucleon-hole state with $T_f=T_i+\frac{1}{2}$, and well defined nuclear spin and parity. (The last point deserves a further remark, since the spin-orbit coupling is known to be small for the Λ in the nucleus.¹⁻¹³ 1 Λ -1h configurations in hypernuclei are experimentally identified, and it is completely meaningful to also specify the J^P quantum numbers of the final hypernuclear levels.¹⁶⁻¹⁸ We shall find that for some configurations cer-

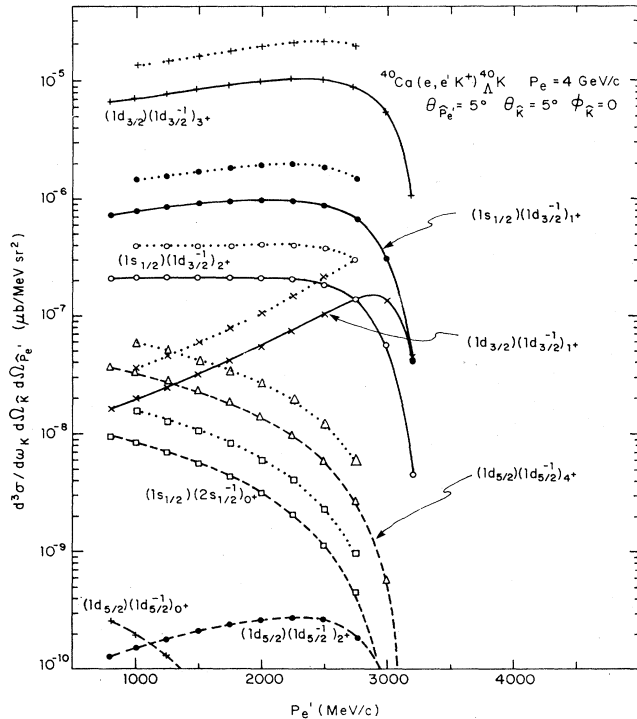


FIG. 3. Energy dependence of exclusive cross sections of the $(e, e'K^+)$ reaction on ${}^{40}\text{Ca}$, using set II of constants in Table I. We present results for deeply-bound Λ states and substitutional states, spin-flip and non-spin-flip. The outgoing electron momentum is varied, keeping p_e , θ_{p_e} , $\theta_{\hat{K}}$, and $\phi_{\hat{K}}$ constants. The calculations are performed using the form factor vertex function of Eq. (9). The dotted curves, given for comparison, are calculations based on a pointlike $K\Lambda p$ vertex ($\Lambda \rightarrow \infty$).

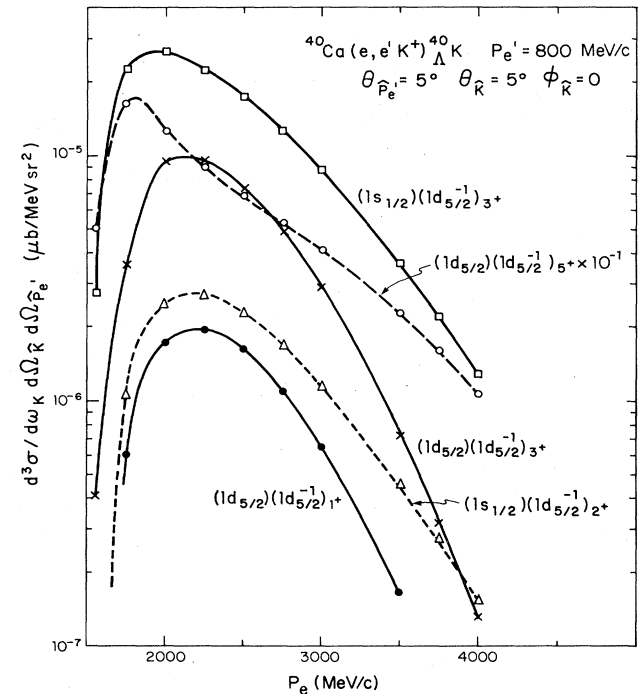


FIG. 4. Energy dependence of the $(e, e'K^+)$ reaction leading to a deeply-bound Λ or to substitutional levels in the ${}^{40}\text{K}$ hypernucleus. The incoming beam energy is varied while holding $p_e' = 800$ MeV/c, $\theta_{p_e} = 5^\circ$, $\theta_{\hat{K}} = 5^\circ$, and $\phi_{\hat{K}} = 0$ constants. Only spin-flip levels are shown. We use set II from Table I, and Eq. (9).

tain J values are more strongly excited than others. In any case, the total strength of the 1Λ - $1h$ configuration can be found by summing over all possible J values.)

B. Threshold ($e, e'K^+$)

Exclusive threshold cross sections for this reaction are generally measurable, but are quite small, because they involve low kaon momenta and relatively large momentum transfers to the nucleus, $Q \sim 400$ – 600 MeV/c. Only spin-flip states are appreciably excited, while non-spin-flip cross sections are too small to be measured *at threshold*.

As is well known, the cross section drops very rapidly with increasing the angle of the outgoing electron ($\theta_{p'_e}$). This has recently been demonstrated also in the (kinematically similar) ($e, e'\pi$) reaction.²⁶ We shall thus present results for $\theta_{p'_e} = 5^\circ$, where the cross section is not yet overly reduced.

In Fig. 2 we present exclusive differential cross sections for the excitation of the $J^P = 1^+, T = \frac{1}{2}$ level in ${}_{\Lambda}^1B$ for three different 1Λ - $1h$ configurations. We show calculations using three different form factors. The calculations with the form of Eq. (10) (the solid curve) coincide with those based on using Eq. (11) and $\Lambda = 900$ MeV around high Q^2 ($Q \approx 550$ – 650 MeV/c), and differ at low Q^2 , where the term $-m_{K^+}^2$ has an appreciable effect, lowering the cross sections. At very high Q the results again differ, because Eq. (10) represents a dipole form factor, while Eq. (11) is of the monopole type. Calculations with the form of Eq. (11) and $\Lambda = 1200$ MeV (represented in Fig. 2 by the dashed-dotted curve) coincide with the solid curve at low values of Q^2 ($Q \approx 300$ – 400 MeV/c), where $\Lambda^2/Q^2 \gg 1$ and $m_{K^+}^2$ is too small compared with Λ^2 to make a large difference. At high Q the higher cutoff makes the cross section higher than the $\Gamma_v(Q^2) = (1 - Q^2/\Lambda^2)^{-2}$ ($\Lambda = 900$ MeV) case, as should be expected from a higher cutoff parameter.

In this threshold case we mainly see, as in Fig. 2, the high-momentum tail of the wave functions. It is found that positive- and negative-, natural- and unnatural-parity states are equally well excited by the reaction. Using the various sets of Table I, we found that only *one coupling constant*, $g_{K\Lambda p}$, dominates the behavior of the cross section. The results shown in Fig. 2 were calculated using set II of constants in Table I.

We have also checked the ϕ_K dependence of the reaction cross section. This turns out to be relatively unimportant for threshold kaon production (of the order of $\pm 10\%$), but becomes more significant for higher kaon momenta, as can be expected.

C. Medium- and high-energy kaon production

While threshold electroproduction was sensitive only to the high-momentum tail of the wave functions, higher kaon momenta permit smaller momentum transfers (for a small angle θ_K). As a result, more structure is revealed (Figs. 3 and 6–8). In Fig. 2, we already observe effects due to different polynomials up to second order in Q^2 .

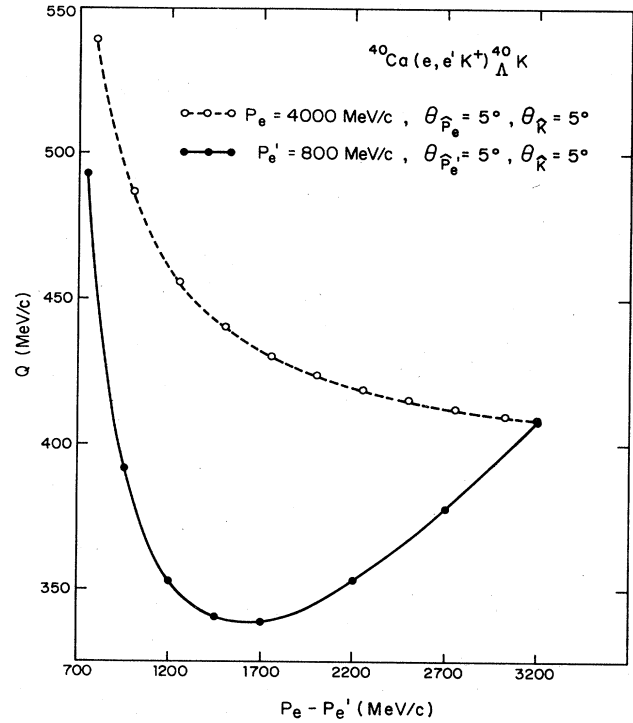


FIG. 5. The momentum transfer Q against the electron energy loss $p_e - p'_e$ for the kinematical conditions of Figs. 3 (the dashed line with open circles) and 4 (the solid line with full circles).

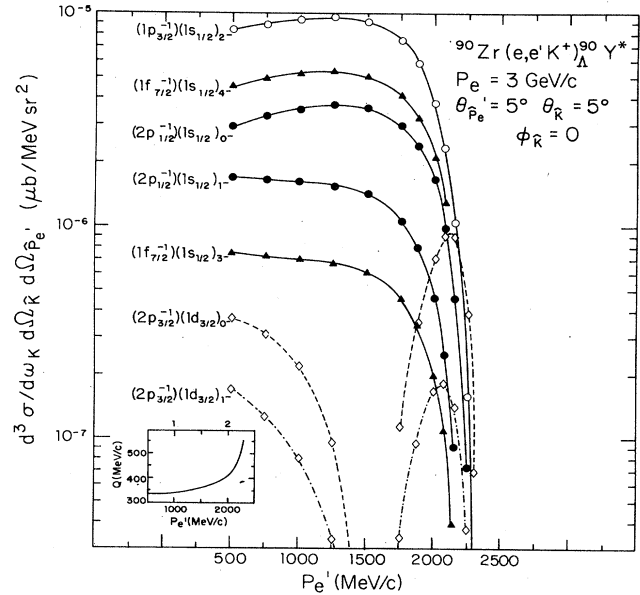


FIG. 6. Exclusive cross sections of the ($e, e'K^+$) reaction on ${}^{90}\text{Zr}$, using set II of Table I and Eq. (9). The insert on the lower-left corner shows the momentum transfer Q vs the outgoing electron momentum p'_e .

Results for higher momenta (note that we are still using the same nonrelativistic amplitude and nuclear dynamics, which may not be a good approximation any more) and for excitations of both spin-flip and non-spin-flip levels in ${}^{40}_{\Lambda}\text{K}$ are given in Fig. 3. The latter will become measurable for high-enough beam energies. The results of Fig. 3 refer to deeply bound Λ (in the $1s$ state) and substitutional ($nlj^{-1}nlj$) states. We calculated for a constant beam energy and varied the outgoing beam energy, keeping the angles fixed. A similar calculation was also carried out for a constant outgoing electron momentum (which is experimentally less realistic) $p'_e = 800$ MeV/c, where the incoming beam energy was varied. Results pertaining to spin-flip levels for $\theta_{p'_e} = 5^\circ$, $\theta_{\hat{K}} = 5^\circ$, and $\phi_{\hat{K}} = 0$ are shown in Fig. 4. The shapes of the graphs in Figs. 3 and 4 are largely determined by the momentum transfer, as can be seen from a comparison with Fig. 5. [Note that the x axis in Fig. 5 is $(\text{const} - p'_e)$ for the case of Fig. 3 and $(p_e - \text{const})$ in the case of Fig. 4.]

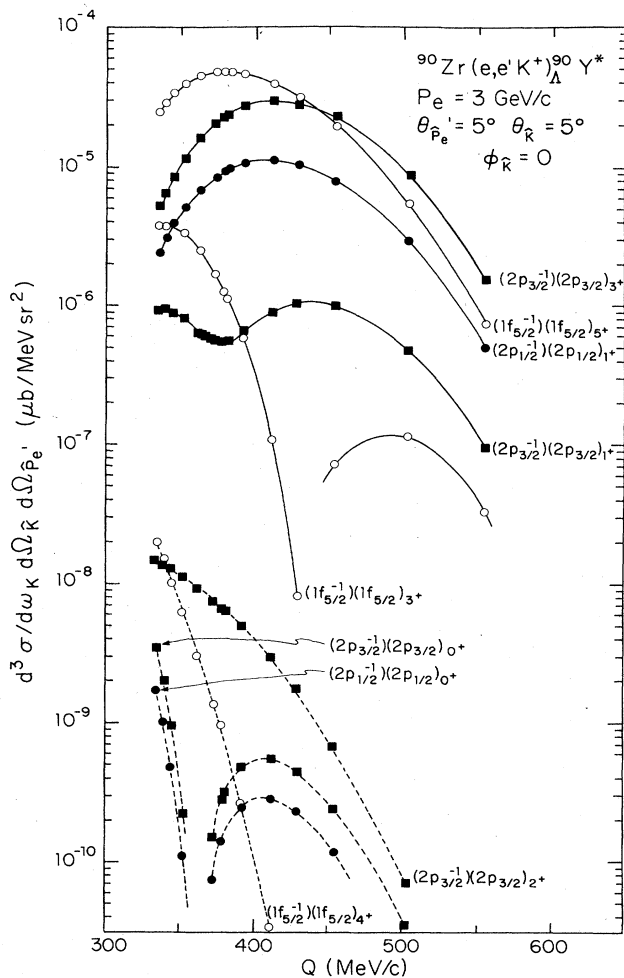


FIG. 7. Exclusive cross sections of the $(e,e'K^+)$ reaction on ${}^{90}\text{Zr}$, using set II of Table I and Eq. (9), as a function of the momentum transfer Q . The relationship between Q and p'_e is given in Fig. 6.

D. Heavier nuclei

In this subsection we discuss heavy nuclei because they are important for studying the (weak) decay of Λ hypernuclei. While mesonic decay modes are dominant in very light hypernuclei, the nonmesonic modes ($\Lambda + N \rightarrow N + N$) are dominant in heavier ones. Studies of such decays are important for the understanding of the four fermion weak interaction; since we anticipate such studies,³⁹ we believe it might be useful to present here results for heavy hypernuclei.

Cross sections for hypernuclear level excitations in ${}^{90}\text{Zr} \rightarrow {}^{90}_{\Lambda}\text{Y}^*$ and ${}^{208}\text{Pb} \rightarrow {}^{208}_{\Lambda}\text{Tl}^*$ are shown in Figs. 6–8. The magnitudes of the cross sections are similar to those calculated for ${}^{40}\text{Ca}$, but more structure is revealed, as lower values of momentum transfer are reached, especially for ${}^{90}\text{Zr}$ (Figs. 6 and 7). The correspondence between Figs. 6 and 7 is made clear through the insert in Fig. 6, showing the momentum transfer Q vs p'_e for this case. Very high spin states are excited with large cross sections (see Fig. 8), but those are probably not readily detectable (experimentally) in nuclei such as ${}^{208}\text{Pb}$.

VI. INCLUSIVE HYPERNUCLEAR EXCITATIONS

In this section we study the inclusive $(e,e'K^+)$ reaction, where a sum over all final nuclear states is performed. The inclusive process will, of course, have much higher cross sections, and will probably be studied first when the reaction is performed in future experiments. It is well

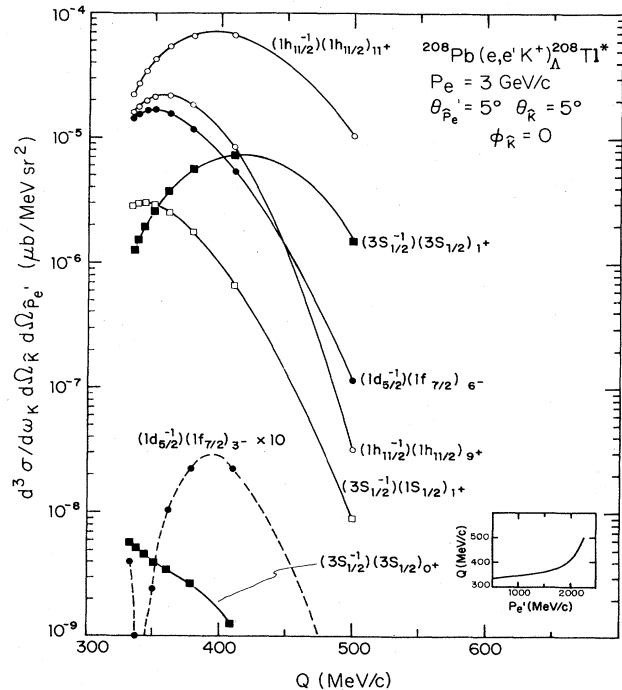


FIG. 8. As Fig. 7, with the insert at the lower right corner as in Fig. 6, but for ${}^{208}\text{Pb}$.

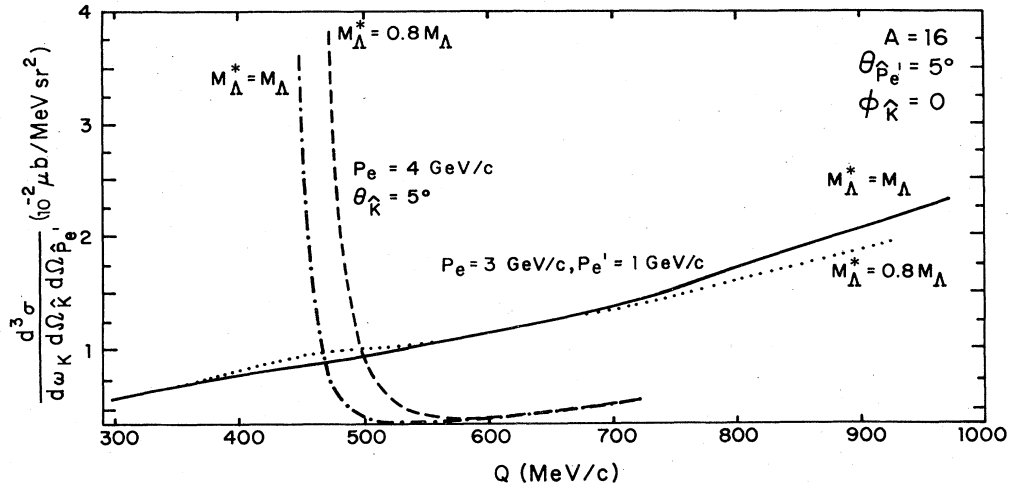


FIG. 9. Inclusive cross sections on ^{16}O , using set II of constants from Table I and the form factor of Eq. (10). Results are shown for $M_{\Lambda}^* = M_{\Lambda}$ and $0.8 M_{\Lambda}$, for two different kinematical setups (p_e' or $\theta_{\hat{K}}$ vary).

known that the inclusive process is governed by continuum excitations.^{26,40} In a previous work⁴¹ we have shown that for momentum transfers above 300 to 400 MeV/c it is possible to apply the closure approximation very reliably in summing over final nuclear states. Using this, we sum over final states $|f\rangle$ in the expression for the exclusive cross section and find a single-nucleon and a two-nucleon contribution. Here, we analyze the one-body part, dropping the spin correlation term, which is expected to be small.⁴² Also, we note that for inclusive cases the consideration of plane-wave outgoing particles is even more appropriate; since we sum over all possible final nuclear states, no optical (nuclear) distortion is needed for the K^+ meson.

Even for spin-saturated nuclei the calculation is lengthy because of the large number of terms in J_{μ} . For such nuclei the resulting cross section is determined by the

kinematics. [Interestingly, this kinematics places an upper limit on the value of $\theta_{\hat{p}_e'}$ for low kaon momenta.

This limit, resulting from the relatively large mass of the kaon and difference in masses between the hypernucleus $_{\Lambda}A^*$ and the parent nucleus A , is not present, for example, when one considers the $(e, e'\pi)$ reaction. It is also not present for high-energy kaons.]

The inclusive cross sections are presented in Fig. 9 against the momentum transfer Q at $\theta_{\hat{p}_e'} = 5^\circ$, $\phi_{\hat{K}} = 0$ for two different values of the Λ effective mass: $M_{\Lambda}^* = M_{\Lambda} = 1115.7$ MeV and $M_{\Lambda}^* = 0.8 M_{\Lambda}$. We show results for $\theta_{\hat{K}} = 5^\circ$ and various values of p_e' (dashed-dotted and dashed curves), as well as $p_e' = 1$ GeV where $\theta_{\hat{K}}$ varies (full and dotted curves). While the form factor of Eq. (10) is used in the calculations for Fig. 9, no form factor (i.e.,

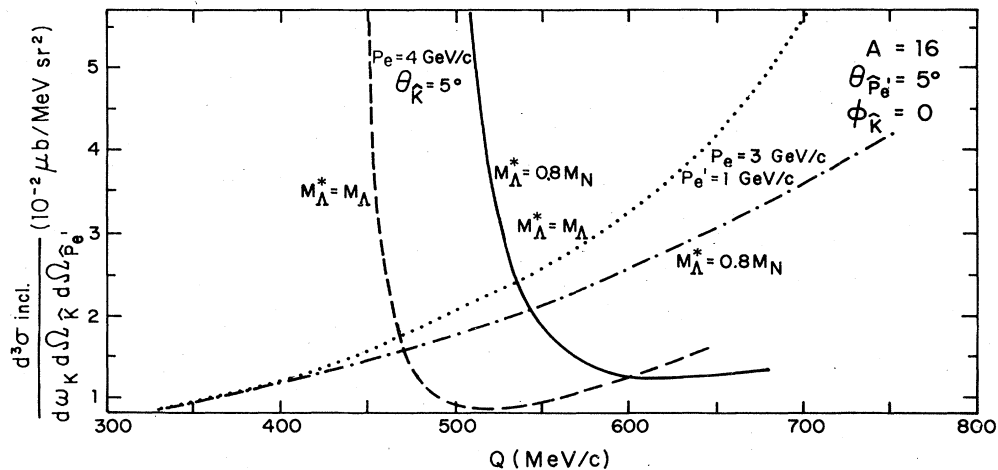


FIG. 10. Inclusive cross sections on ^{16}O , using set II of constants from Table I and pointlike vertices (no form factor). Results are shown for $M_{\Lambda}^* = M_{\Lambda}$ and $0.8 M_N$ for the two kinematical setups as in Fig. 9.

pointlike vertices) were introduced when calculating for Fig. 10. In Fig. 10 we show results for $M_{\Lambda}^* = M_{\Lambda}$ and $M_{\Lambda}^* = 0.8M_N$. All cross sections are two to three orders of magnitude higher than the exclusive ones. The cross sections are mainly governed by the leading coupling constant $g_{K\Lambda p}$ to within $\pm 10\%$. We thus conclude that very accurate calculations and measurements will be necessary to determine the other constants of Table I. The dependence on the azimuthal angle $\phi_{\vec{k}}$ (out of the $\mathbf{p}_e\text{-}\mathbf{p}'_e$ plane) is relatively weak (of the order of a few percent) even for the high beam energies considered here.

These results indicate the measurability of the $(e, e'K^+)$ reaction cross sections.⁴³ Once these measurements become accurate enough, they will throw new light on a

large spectrum of problems in nuclear and intermediate-energy physics.

ACKNOWLEDGMENTS

It is a pleasure to acknowledge Julian V. Noble for suggesting the subject of this work and for encouragement and help. J. M. Eisenberg, H. J. Weber, C. B. Dover, and H. Fearing contributed a lot in discussions and suggestions during the various stages of this study. Thanks are due to J. S. McCarthy for estimating counting rates on the cw CEBAF with the cross sections calculated here. I am thankful to K. Amos for useful correspondence concerning the distortion of the K^+ meson. This work was supported by the National Science Foundation under Grant No. PHY-A2-00578-01.

¹C. B. Dover and G. E. Walker, Phys. Rep. **89**, 1 (1982).

²G. Ya. Korenman and V. P. Popov, Phys. Lett. **40B**, 628 (1972); B. Povh, Annu. Rev. Nucl. Sci. **28**, 1 (1978).

³A. Gal, in *Common Problems in Low- and Medium- Energy Nuclear Physics*, edited by B. Castel, B. Goulard, and F. C. Khanna (Plenum, New York, 1979).

⁴C. B. Dover, Nucl. Phys. **A335**, 227 (1980).

⁵B. Povh, Nucl. Phys. **A335**, 233 (1980).

⁶R. H. Dalitz, Nucl. Phys. **A354**, 101c (1981).

⁷Proceedings of the Second Kaon Factory Physics Workshop, Vancouver, 1981, edited by R. M. Woloshyn and A. Strathdee, TRIUMF Report No. TRI-81-4, 1981.

⁸C. B. Dover, Nucl. Phys. **A374**, 359c (1982).

⁹P. D. Barnes, Nucl. Phys. **A374**, 415c (1982).

¹⁰C. B. Dover and A. Gal, in *Progress in Particle and Nuclear Physics*, edited by D. H. Wilkinson (Pergamon, Oxford, 1984), Vol. 12, p. 171.

¹¹Proceedings of the International Conference on Hypernuclear and Kaon Physics, Heidelberg, 1982, edited by B. Povh.

¹²B. Povh, in *Proceedings of the International School of Intermediate Energy Nuclear Physics, Verona, 1981 (Third Course)*, edited by R. Bergere, S. Costa, and C. Schaerf (World Scientific, Singapore, 1982).

¹³C. B. Dover, in Proceedings of the Second LAMPF II Workshop, Los Alamos, 1982, edited by H. A. Thiessen, T. S. Bhatia, R. D. Carlini, and N. Hintz, Los Alamos National Laboratory Report No. LA-9572-C, 1982, p. 62; G. E. Walker, *ibid.*, p. 202; M. May, *ibid.*, p. 302.

¹⁴C. B. Dover *et al.*, Phys. Lett. **89B**, 26 (1979).

¹⁵V. N. Fetisov, M. I. Kozlov, and A. I. Lebedev, Phys. Lett. **38B**, 129 (1972).

¹⁶C. B. Dover, L. Ludeking, and G. E. Walker, Phys. Rev. C **22**, 2073 (1980).

¹⁷A. M. Bernstein, T. W. Donnelly, and G. N. Epstein, Nucl. Phys. **A358**, 195c (1981).

¹⁸S. S. Hsiao and S. R. Cotanch, Phys. Rev. C **28**, 1668 (1983); Bull. Am. Phys. Soc. **28**, 747 (1983); **29**, 646 (1984).

¹⁹S. R. Cotanch and S. S. Hsiao, in *Intersections Between Particle and Nuclear Physics*, Proceedings of The Conference on the Intersections Between Particle and Nuclear Physics, AIP Conf. Proc. No. 123 (AIP, New York, 1984), p. 778.

²⁰J. V. Noble, and R. R. Whitney, Conference on New Horizons in Electromagnetic Physics, University of Virginia, Charlottesville, Virginia, 1982 (this paper was not included in the

published proceedings by mistake); and private communication.

²¹Joseph Cohen, Phys. Lett. **153B**, 367 (1985); Joseph Cohen and J. V. Noble, Bull. Am. Phys. Soc. **29**, 1052 (1984).

²²J. V. Noble, Phys. Rev. Lett. **46**, 412 (1981); P. D. Zimmermann, Phys. Rev. C **26**, 265 (1982).

²³J. P. Vary, Nucl. Phys. **A418**, 195c (1984).

²⁴N. Anantaraman *et al.*, Phys. Rev. Lett. **52**, 1409 (1984).

²⁵C. Djalali *et al.*, Nucl. Phys. **A410**, 399 (1983).

²⁶Joseph Cohen and J. M. Eisenberg, Phys. Rev. C **28**, 1309 (1983).

²⁷H. Thom, Phys. Rev. **151**, 1322 (1966).

²⁸J. D. Bjorken and S. D. Drell, *Relativistic Quantum Mechanics* (McGraw-Hill, New York, 1964).

²⁹T. K. Kuo, Phys. Rev. **129**, 2264 (1963).

³⁰O. Dumbrajs *et al.*, Nucl. Phys. **B216**, 277 (1983).

³¹M. Bozoian, J. C. H. van Doremalen, and H. J. Weber, Phys. Lett. **122B**, 138 (1983).

³²M. M. Nagels, T. A. Rijken, and J. J. deSwart, Phys. Rev. D **15**, 2547 (1977).

³³F. Dydak *et al.*, Nucl. Phys. **B118**, 1 (1977).

³⁴N. Isgur and G. Karl, Phys. Rev. D **21**, 3175 (1980).

³⁵M. Bozoian and H. J. Weber, Phys. Rev. C **28**, 811 (1983).

³⁶N. Isgur and G. Karl, Phys. Rev. D **18**, 4187 (1978); **19**, 2653 (1979).

³⁷H. Fearing, private communication. I am grateful to Harold Fearing for pointing out this problem to me, and to Julian Noble for a discussion of the problem.

³⁸J. M. Eisenberg and W. Greiner, *Microscopic Theory of the Nucleus* (North-Holland, Amsterdam, 1972).

³⁹B. H. J. McKellar and B. F. Gibson, Phys. Rev. C **30**, 322 (1984).

⁴⁰Joseph Cohen and J. M. Eisenberg, Nucl. Phys. **A395**, 389 (1983).

⁴¹See Ref. 40, Sec. 3.

⁴²G. Orlandini, M. Traini, and F. Dellagiacoma, Nuovo Cimento **76A**, 246 (1983); F. Dellagiacoma, R. Ferrari, G. Orlandini, and M. Traini, Phys. Rev. C **29**, 777 (1984).

⁴³We have calculated for plane-wave electrons and kaons. Two types of distortions should be considered in a more complete calculation: (a) The optical (strong) absorption of the K^+ meson interacting with the nucleus, and (b) the Coulomb distortion of the (negatively charged) electrons and the (positive) kaon. The optical (nuclear) absorption should only be con-

sidered for the *exclusive* excitations, because in the *inclusive* case we have summed over all possible final states and no optical distortions are present (see also Refs. 40 and 26). In the former case, it is well established that distortion effects on ^{12}C and other light nuclei are very small, of the order of 8–25 %, as determined by K. Amos and F. DiMarzio, Phys. Rev. C **29**, 1914 (1984); P. B. Siegel, W. B. Kaufmann, and W. R. Gibbs, Bull. Am. Phys. Soc. **30**, 766 (1985); Phys. Rev. C **30**, 1256 (1984). This is, of course, a result of the relatively small and uniform (as a function of energy) $\text{K}^+\text{-N}$ cross section, corresponding to the mean free path of approximately 5 fm in nuclear matter. The results for nuclei heavier than Ca are also not expected to be *very* sensitive to the optical distortion (K. Amos, private communication). In view of the crude calculation presented here, we shall just estimate the effect of distortion on heavier nuclei. This distortion can be calculated extremely reliably in the eikonal approximation (Ref. 16). We further assume an overall attenuation factor, whereby angular

distributions are affected by the distortion mainly in overall magnitude and not in shape [P. B. Siegel, W. B. Kaufmann, and W. R. Gibbs, Phys. Rev. C **30**, 1256 (1984); H. C. Chiang and J. Hüfner, Phys. Lett. **84B**, 393 (1979)]. This only provides a crude estimate, and we hope to improve our results in future works. In any case, the uncertainties of the model do not permit an exact estimate of the cross sections, and the distortion is, after all, quite small. We use the total K^+N cross section as given in Ref. 16, that is, around 15 mb and disregard the real part of the K^+N scattering amplitude [$\text{Re}f_{\text{K}^+\text{N}}(0^\circ)$]; as Dover, Ludeking, and Walker (Ref. 16) indicate, cross sections are almost independent of $\text{Re}f_{\text{K}^+\text{N}}(0^\circ)/\text{Im}f_{\text{K}^+\text{N}}(0^\circ)$. This indicates an attenuation of about 50–70 % in the ^{208}Pb cross section from optical absorption. The Coulomb distortion of the electrons and the kaon is probably important because of the high charge number of ^{208}Pb , and will be considered elsewhere.